applied sciences

MDPI

Article

Development of a Flexible Thin Wearable Device for Tuning Temperature, Humidity, and Surface Friction on Its Surface

Toshihiro Nishimura [1,*], Natsuko Kuramata [2], Seita Nojiri [2], Yuki Horiuchi [2], Kenjiro Tadakuma [3] and Tetsuyou Watanabe [1,*]

1 Faculty of Frontier Engineering, Institute of Science and Engineering, Kanazawa University, Kakuma-Machi, Kanazawa 9201192, Ishikawa, Japan
2 Graduated School of Natural Science and Technology, Kanazawa University, Kakuma-Machi, Kanazawa 9201192, Ishikawa, Japan
3 Graduation School of Information Sciences, Tohoku University, Sendai 9808579, Miyagi, Japan
* Correspondence: tnishimura@se.kanazawa-u.ac.jp (T.N.); twata@se.kanazawa-u.ac.jp (T.W.)

Abstract: This study proposes a wearable device that adapts its surface conditions to maximize user comfort using novel strategies to change its temperature, humidity, and friction. The device consists of three functional units, namely heating, liquid injection, and dry-air blowing units, composed of flexible materials and thin structures. Owing to its flexibility and thickness, it can be installed on garments. The surface conditions change according to the collaborative actions of the three functional units. The temperature is increased using the heating unit and decreased using both the liquid-injection and dry-air blowing units. Humidity is increased and decreased by the liquid-injection and dry-air blowing units, respectively. Finally, the friction of the contact surface area of the device with human skin is increased and decreased using the liquid-injection and dry-air blowing units, respectively. These methodologies are experimentally validated under different environmental conditions. The validation reveals that the injection of a liquid (deionized water) increases surface friction, whereas blowing air decreases friction; in particular, the presence of granular objects is effective at reducing friction. In addition, the environmental conditions of temperature and humidity influence the degree of increase or decrease, primarily because the amount of water is varied to change the humidity, lower the temperature, and increase friction: vaporization heating lowered temperature and adhesion force of water increased friction. The temperature, humidity, and kinetic friction of the wearable device range from −2.6 to +5.0 °C, −19% to +12%, and −73% to +45%, respectively.

Keywords: clothing; variable friction; variable humidity; variable temperature; wearable devices

Citation: Nishimura, T.; Kuramata, N.; Nojiri, S.; Horiuchi, Y.; Tadakuma, K.; Watanabe, T. Development of a Flexible Thin Wearable Device for Tuning Temperature, Humidity, and Surface Friction on Its Surface. *Appl. Sci.* **2023**, *13*, 8352. https://doi.org/10.3390/app13148352

Academic Editor: Paolo Visconti

Received: 8 June 2023
Revised: 13 July 2023
Accepted: 18 July 2023
Published: 19 July 2023

1. Introduction

This study proposes a novel wearable device for comfortable human activities. It can be installed on flexible fabrics, such as clothes, and certain parameters, such as the temperature, humidity, and friction of the surface area of the device (on clothes) in contact with the human body, can be tuned as needed. Thermal comfort is the balance between the metabolic heat generated by the human body and its heat loss to the environment [1,2]. Thus, thermoregulation or optimization of the temperature and humidity in the contact area is important [3]. When dressing and undressing, the skin can be damaged if the direct friction between the clothes and the surface of the human body is excessively high. However, sufficiently high friction between the clothes and skin is required to hold and support the human body comfortably. Not only thermoregulation but also the friction experienced in the contact area are important for comfortable human support. However, no attempt has been made to address friction in wearable devices. Figure 1 illustrates the main goal of this study. The objective is to develop a device with a flexible, thin structure that can change the temperature, humidity, and friction between clothes and the human skin and can be worn on garments. The control and source components are installed to drive the developed device. Portability is obtained through including an electrical battery and a portable air source, as reported in [4]. This study attempted to develop a core device to achieve this goal. Note that the air and electrical sources used in this study are not portable. The first challenge involves changing the contact friction with changes in temperature and humidity in the contact area. The second challenge involves developing a thin and flexible device that can be installed on clothing, including components that actuate the changes. To achieve this, the units that control changes in temperature, humidity, and friction are built using only compressed air and electric wires. The use of thin and flexible air tubing eliminates the need for rigid components in clothing, thereby creating a lightweight, non-rigid device. The change in contact friction is a key breakthrough proposed herein. A liquid with high surface tension is directly sprayed between the device and the skin, thus increasing the friction. Inspired by the Venturi effect, herein, this study developed a thin and flexible spraying mechanism using a flexible material (silicone) to eliminate the need to pump the liquid. The contact friction is lowered through forming an air-lubricated layer on the clothes by means of blowing dry air, which facilitates the drying of the contact areas wetted by the spray. In addition, spray is used to increase the humidity. The third challenge involves minimizing the number of actuators required. Temperature reduction is achieved through combining liquid spraying with dry air blowing via heat vaporization. These principles allow for the control of changes in temperature, humidity, and friction in the contact area between the device and the human skin using only compressed air. This also allows the use of a single power source and avoids the use of rigid components, such as electrical motors. Heating is achieved using the Joule effect of thin and flexible electric wires.

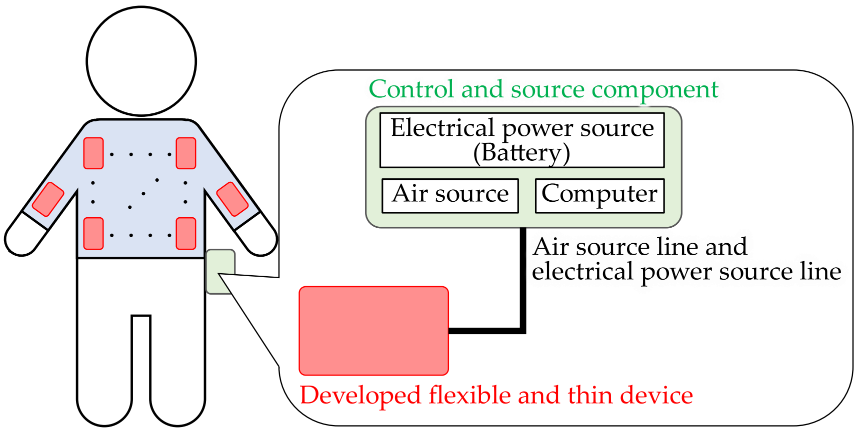

Figure 1. Illustration of the device developed in this study.

The thermal management of the human body is important for comfortable human activities. Several studies have proposed different mechanisms that can change the surface temperature using various strategies, such as fluid flow, phase change, and electrical power [5]. Table 1 presents a comparison between this work and existing works that can tune the temperature, humidity, or friction. Kotagami et al. developed a liquid cooling system that uses a soft, thermally conductive silicone–aluminum composite tube [6]. Guo et al. designed a liquid-cooling-based garment that fed cold water into the human body using an electrical pumping system and evaluated it in a hot environment [7]. A phase change mechanism that absorbs or releases thermal energy was proposed as a temperature change mechanism [8]. Bühler et al. investigated the heat-protection performance of several phase-change materials [9]. Several heating and cooling systems driven by electrical power, using electrical heating elements [10–12] and thermoelectric materials [13–15], have been proposed. The humidity of the environment is also effective for improving comfortability. Although several commercial devices can change humidity [16,17], they have been adapted to change the humidity of garments. Moreover, several studies have proposed mechanisms that can change surface friction, particularly in the field of robotics [18–29]. Our research group also developed a variable-friction system through injecting a lubricant onto the surface of a mechanism [30,31]. Although the previous system aimed to reduce friction, the aim of the current study is to increase it because variable friction is necessary for stable human support. This literature review reveals the different mechanisms or strategies that are currently available or underway to enable the tuning of the conditions set in our aim: temperature, humidity, and friction. However, no attempt has been made to realize a device that can change all these conditions using a flexible and thin structure that can be worn in garments, as shown in Table 1. Thus, this study proposes the development of such a device while optimizing the number of actuating units required. The contribution of this study is the development of a flexible thin device that can tune the temperature, humidity, and friction of a target surface. It should be noted that the aim of the developed device is not to independently tune the temperature, humidity, and friction, because the aim of the developed device is to provide comfort for human activity. For example, a simultaneous reduction in humidity and friction improves the breathability of garments.

Table 1. Comparison with existing works.

	Tuning the Temperature		Tuning the Humidity		Tuning the Friction
	Increasing	Decreasing	Increasing	Decreasing	Increasing or Decreasing
This work	**Yes**	**Yes**	**Yes**	**Yes**	**Yes**
[6]	-	Yes	-	-	-
[7]	-	Yes	-	-	-
[10]	Yes	-	-	-	-
[11]	Yes	Yes (passive)	-	-	-
[12]	Yes	-	-	-	-
[13]	-	Yes	-	-	-
[14]	-	Yes	-	-	-
[16]	-	-	Yes	Yes	-
[17]	-	-	Yes	Yes	-
[18]	-	-	-	-	Yes
[19]	-	-	-	-	Yes
[20]	-	-	-	-	Yes
[21]	-	-	-	-	Yes
[22]	-	-	-	-	Yes
[23]	-	-	-	-	Yes
[24]	-	-	-	-	Yes
[25]	-	-	-	-	Yes
[26]	-	-	-	-	Yes
[27]	-	-	-	-	Yes
[28]	-	-	-	-	Yes
[29]	-	-	-	-	Yes
[30]	-	-	-	-	Yes
[31]	-	-	-	-	Yes

2. Units for Changing Conditions

2.1. Functional Requirements

The developed device should incorporate the following functional requirements: (1) allow the tuning of temperature, humidity, and friction in the contact area between the fabric and target surface (human skin); (2) be a thin and flexible structure that can be worn on clothes; and (3) have no electrical motors.

2.2. Overview of the Developed Device

Figure 2 shows the developed device, which can change the temperature, humidity, and friction in the contact area between itself and a target surface (the human body or skin). It consists of liquid-injection, dry-air blowing, and heating units. The components used to fabricate the units and their flexibilities are listed in Table 2. The device was sufficiently flexible and thin for installation on clothing, as presented in Figure 2 and Table 1. It relies on a single air source, an electrical power source, several solenoid valves, and a computer to control the valves. A power supply with up to 2.5 W is required to operate the heating unit, whereas a power of only 0.1 W is sufficient to drive the valves and portable air source (a small gas cylinder). Mobile batteries can supply this power easily. The entire system, including the developed device and the peripheral tools to operate it, is portable.

Table 2. Materials of the developed unit.

	Component	Material/Property	Flexibility	Specifications (Model Name, Manufacturer)
Heating unit	Electrical heating wire	Nichrome	Flexible	Wire diameter: 0.26 mm (HK-NK05H, Asahi electric Co., Ltd., Osaka, Japan)
	Wire cover	Silicone	Flexible (Shore A50)	Outer diameter: 2 mm (MGJG-1 × 2, Monotaro, Hyogo, Japan)
	Electrical cable	-	Flexible	Diameter of the electrical wire: 0.1 sq (U-0817, Suzuden Corporation, Tokyo, Japan)
Liquid-injection unit	Main body	Silicone (Dragon skin 10)	Flexible (Shore A10)	(Dragon skin 10, Smooth-On, Macungie, PA, USA)
	Liquid-storing object	Cotton	Flexible	Size: 100 mm × 100 mm (31,413, Worldjb Co., Ltd., Tokyo, Japan)
	Air tube	Silicone	Flexible (Shore A50)	Outer diameter: 2 mm (MGJG-1 × 2, Monotaro)
Dry-air blowing unit	Air tube	Silicone	Flexible (Shore A50)	Outer diameter: 2 mm (MGJG-1 × 2, Monotaro)
	Cotton bag	Cotton	Flexible	-
	Granular objects	Unpolished rice	Flowable	-
	Inline air filter	-	(Rigid) *	Diameter: 22 mm, length: 115 mm (IAD3-N20-T4, kitz micro filter corporation, Nagano, Japan)

* Installed separately from clothes.

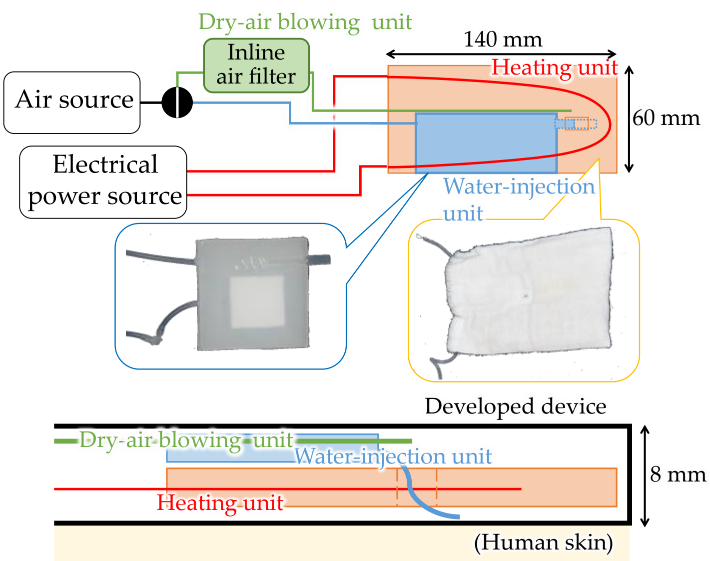

Figure 2. Schematic of the developed device.

3. Principles of the Tuning the Temperature, Humidity, and Friction

3.1. Structure of the Developed Units

3.1.1. Liquid-Injection Unit

Figure 3 shows the structure of the liquid injection unit. It consists of an airflow path with a throttled section (orifice), and a path that bifurcates from the orifice and connects to the liquid storage space within the cotton. The structure was molded using a flexible material (Dragon Skin 10). The principle of the Venturi effect is used to inject the liquid stored within the cotton onto the contact surface using the input airflow. Using the Bernoulli principle, the difference in the airflow pressure between the wide section and the orifice can be obtained as follows:

$$p_1 - p_2 = \frac{\rho\left(v_2^2 - v_1^2\right)}{2}, \tag{1}$$

where ρ is the density of air; p_1, v_1, and s_1 are the airflow pressure, airflow velocity, and cross-sectional area of the airflow path at the wide section before flowing to the orifice, respectively; and p_2, v_2, and s_2 are the airflow pressure, airflow velocity, and cross-sectional area of the airflow path at the orifice, respectively. If q is the volumetric airflow rate from the air source and is constant in the two sections, the following continuous equation is observed: $q = v_1 s_1 = v_2 s_2$. Considering $v_1 = q/s_1$ and $v_2 = q/s_2$, Equation (1) can be rewritten as follows.

$$p_1 - p_2 = \rho q^2 \left(\frac{1}{s_2^2} - \frac{1}{s_1^2}\right), \tag{2}$$

where $p_1 > p_2$ is satisfied, as $s_2 < s_1$. Hence, a negative pressure is generated in the orifice. This forces the liquid to be ejected from the cotton through the orifice. The ejected liquid is sprayed onto the surface of the unit with airflow. The unit is constructed with soft materials; thus, the negative pressure around the orifice can cause undesired deformation (e.g., inflation around the orifice) in the structure, resulting in reduced performance. To avoid undesired inflation of the flow path around the orifice, the flow path area was sewn with a thread, as shown in Figure 3.

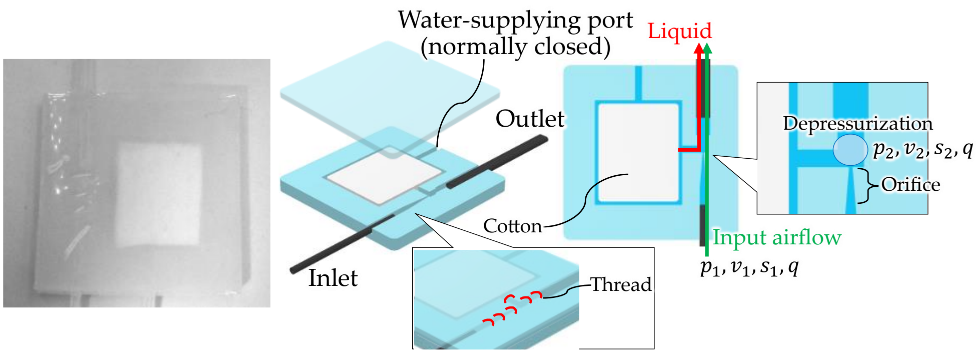

Figure 3. Schematic of the liquid-injection unit.

The performance of the liquid injection unit was experimentally validated using the experimental setup illustrated in Figure 4. In the experiments, the liquid (deionized water) was injected into a paper towel (KimWipes, Kimberly Clark, Irving, TX, USA) through inputting air at a pressure of 0.1 MPa from the air source to the liquid-injection unit. After injecting the liquid for three seconds, the weight of the paper towel was measured, and the amount of the injected liquid was calculated from the difference between the weight of the towel before and after injecting the liquid. The experiment was conducted twice, with a mean amount of injected liquid of 0.6 g between the trials.

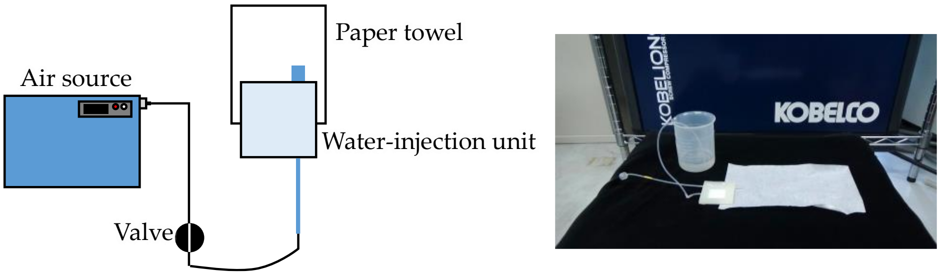

Figure 4. Experimental setup to evaluate the liquid-injection unit.

3.1.2. Dry-Air Blowing Unit

Dry air flowed into the contact area through a pouch that contained granular objects (unpolished rice) through inputting the airflow from the air source through an inline air dryer (IAD3-N40-T4, Kitz microfilter, Nagano, Japan), as shown in Figure 2. The granular materials in pouches play two key roles. The first is to provide an air-lubricated layer: when (dry) air flows into the pouch, the granular materials inside form an air pocket around the contact area, which is enclosed by the pouch and surrounding granular materials; the air pocket creates an air-lubricated layer to reduce the friction on the contact area. The second role is to ensure air movement, even when the developed device is subjected to heavy loads.

3.1.3. Heating Unit

A schematic of the heating unit is presented in Figure 5. It is composed of a nichrome wire covered with a silicone tube. The nichrome wire was routed into a pouch containing granular objects (unpolished rice). A current was applied to the wire using an electrical power source to warm the unit through Joule heating. The pouch, including the granular objects and the silicone tube within it, prevents the high-temperature wire from coming into direct contact with the human body.

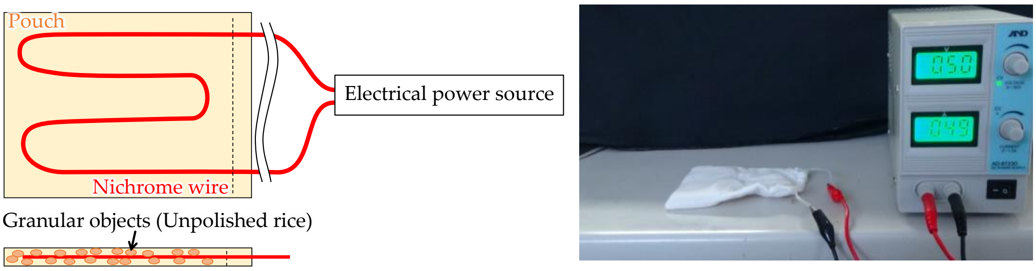

Figure 5. Schematic of the heating unit.

3.2. Principles of Modifying the Conditions

The strategies for changing the contact surface conditions using the device, i.e., tuning the temperature, humidity, and friction using the three units, are as follows.

1. The injection of a liquid with a large surface tension onto the contact area increases the adhesion force [32], which increases friction; when dry air is blown into a cotton bag containing granulated materials, an air pocket or an air-lubricated layer is formed near the contact area, thereby reducing the actual contact area and friction [33].
2. The temperature is increased by the heating unit and decreased via the evaporation-cooling method [8]. A liquid is injected by the liquid-injection unit and vaporized by the dry-air blowing unit.
3. Humidity is increased through spraying a liquid onto the contact area and reduced through blowing dry air into the contact area.

Table 3 summarizes these principles. Note that, as mentioned above, this study does not aim to tune the temperature, humidity, and friction independently.

Table 3. Unit operation settings according to the required surface conditions.

Condition	Change	Heating Mechanism	Liquid-Injection Mechanism	Dry-Air Blowing Mechanism
Temperature	Increase	Yes	-	-
	Decrease	-	Yes	Yes
Humidity	Increase	-	Yes	-
	Decrease	-	-	Yes
Friction	Increase	-	Yes	-
	Decrease	-	-	Yes

4. Evaluation of the Developed Unit

To validate the performance of the developed device in changing its surface contact area properties under several environmental conditions at different temperatures and humidities, various experiments were performed, as summarized in Table 4. In the table, each condition is expressed as "t$\underline{t}$h$\underline{h}$" for temperature $\underline{t}$ [°C] and relative humidity $\underline{h}$ [%]. Each environmental condition was controlled using the experimental setup shown in Figure 6. The developed device and testing tools used to measure the surface properties were placed in an acrylic box. The temperature and humidity within the acrylic box were controlled using an air conditioner and humidifier, as shown in the figure.

Table 4. Summary of the environmental conditions tested to evaluate the developed device.

		Relative Humidity [%]		
		30	**50**	**70**
Temperature [°C]	20	t20h30	t20h50	t20h70
	30	t30h30	t30h50	t30h70

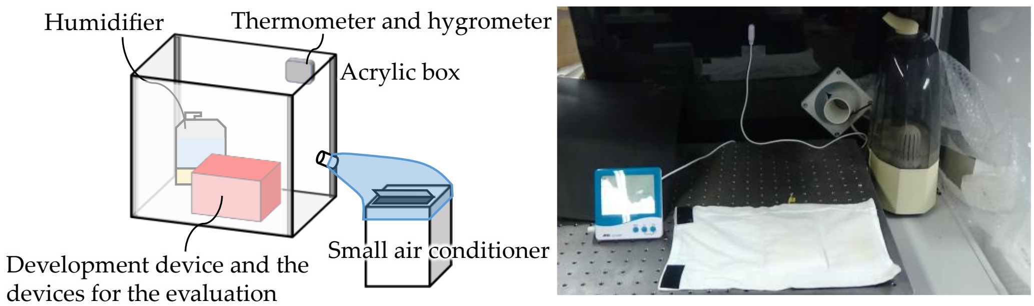

Figure 6. Experimental setup to study the impact of changing the environmental conditions on the developed device.

4.1. Tuning the Temperature

This section presents the evaluation of the performance of increasing/decreasing the temperature on the surface contact area of the device using the heating unit and the evaporation-cooling method, respectively. The experimental setup is illustrated in Figure 7. The first step involved the evaluation of the heating performance. The temperature of the contact area was measured using a thermos-hygrometer under each tested environmental condition while heating for 15 min with a power supply of 2.5 W. The results are presented in Figure 8. Temperatures increased for all conditions tested, albeit at varying rates, depending on the environmental conditions. Under an environmental temperature of 20 °C, the temperature increased by 6.6 °C (heating for 15 min), whereas under 30 °C, it increased by 4.0 °C. It is observed that the lower the environmental temperature, the higher the temperature increase at the contact area. Next, the cooling performance was evaluated using the same experimental setup. The liquid was first sprayed into the contact area by the liquid-injection unit for 1 min. Subsequently, the sprayed liquid was evaporated by the dry-air blowing unit for 2 min. Table 5 presents the results. The temperature of the contact area decreased under all environmental conditions tested. The higher the relative humidity of the environmental conditions, the lower the temperature on the surface of the device, which may be owing to the lower vaporization of the sprayed water under high humidity. These results demonstrated that the developed device could change its temperature under various environmental conditions.

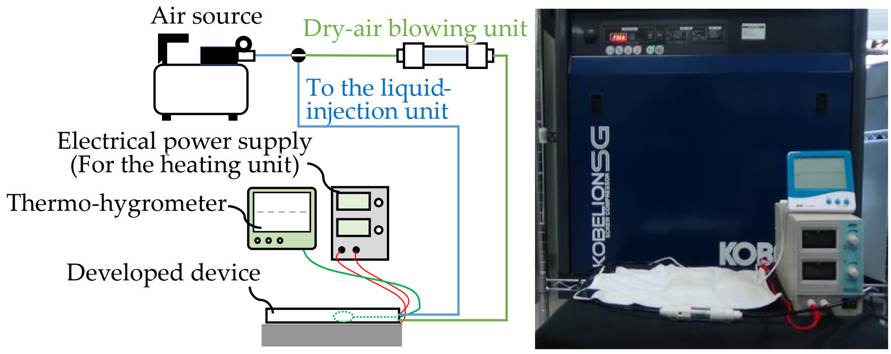

Figure 7. Experimental setup to evaluate the temperature change function.

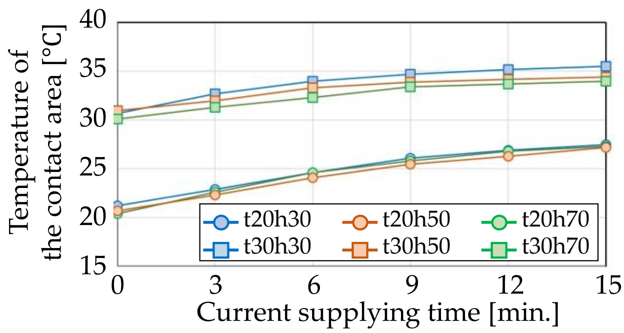

Figure 8. Temperature change of the contact surface with time during heating for each environmental condition tested.

Table 5. Result of temperature lowering function.

	t20h30	t20h50	t20h70	t30h30	t30h50	t30h70
Change of the contact-area-temperature [°C] (Standard deviation)	−4.7 (1.0)	−3.6 (2.1)	−1.5 (0.9)	−12.0 (3.4)	−8.0 (1.6)	−10.8 (2.3)

4.2. Tuning the Humidity

This section presents the evaluation of the performance of humidity tuning on the surface contact area of the device. The experimental setup used was the same as that shown in Figure 7. The changes in the relative humidity of the contact area with respect to the initial conditions were measured after injecting a liquid (deionized water) for 1 min and blowing dry air for 3 min. Table 6 summarizes the experimental results. When the environmental humidity was low, the device increased the humidity of the contact area through injecting the liquid. In contrast, when the environmental humidity was high, the developed device effectively decreased the humidity on the contact surface through blowing dry air. These experiments validated the capability of the developed device to change its surface humidity, although the extent of these changes was intimately affected by the environmental conditions.

Table 6. Result of the function for changing the relative humidity.

	t20h30	t20h50	t20h70	t30h30	t30h50	t30h70
After injecting the liquid [%] (Standard deviation)	+47 (2.1)	+25 (9.5)	+6.3 (2.9)	+41 (10)	+23 (3.8)	+8 (2.0)
After blowing dry air [%] (Standard deviation)	−2 (1.0)	−24 (1.0)	−40 (2.3)	−10 (2.5)	−31 (2.0)	−48 (1.5)

4.3. Tuning the Friction

This section presents the evaluation of the effects of increasing or decreasing friction on the surface contact area of the device. The experimental setup used for these experiments is shown in Figure 9. The maximum static and kinetic friction forces were measured through placing the developed device on top of a bioskin plate (Beaulax H077-002), a model for the human skin, and a load f_n of 130 g on top of the device; subsequently, the bioskin plate and load were pulled using a force gauge, as shown in Figure 9. Measurements were taken after injecting a liquid (deionized water) into the contact area for 1 min to evaluate its ability to increase friction. Subsequently, the frictional force (pulling force) was measured while blowing dry air to evaluate the capability of the device to reduce friction. The pulling speed of the force gauge was set at 1 mm/s. For comparison, the friction force was also measured while the developed device was OFF; this is referred to as the "nominal case." Each experiment was repeated three times under the experimental conditions listed in Table 4. The representative results of these experiments are shown in Figure 10. The maximum static frictional force, $f_{max.st}$, was defined as the initial peak value. The kinetic frictional force, f_{kn}, was defined as the mean value of the friction force for 1 s (1 mm in terms of the pulling displacement) at a steady state after the initial peak. If the steady state time was less than 1 s, the average value was calculated for the entire steady state. Using the measured pulling force ($f_{max.st}$ and f_{kn}) and load applied to the device (f_n), the static and kinetic friction coefficients, μ_{st} and μ_{kn}, were derived as follows.

$$\begin{aligned} \mu_{st} &= f_{max.st}/f_n, \\ \mu_{kn} &= f_{kn}/f_n. \end{aligned} \tag{3}$$

To assess how much friction has changed before and after the friction change, the respective ratios of μ_{st} and μ_{kn} before and after friction change were derived. Figure 11 summarizes the results obtained for all the experiments under different environmental conditions. The ratio of the maximum static and kinetic coefficients of friction after the friction change was compared with that of the nominal case. As expected, the results confirmed that under different environmental conditions, injecting water increased friction, whereas blowing dry air reduced it.

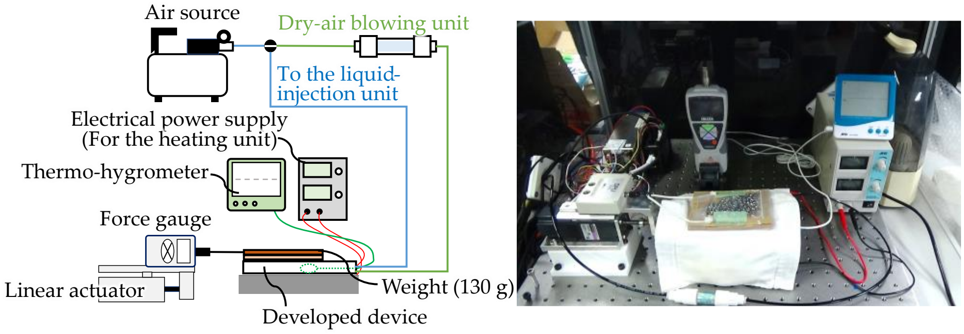

Figure 9. Experimental setup to measure the surface friction coefficient.

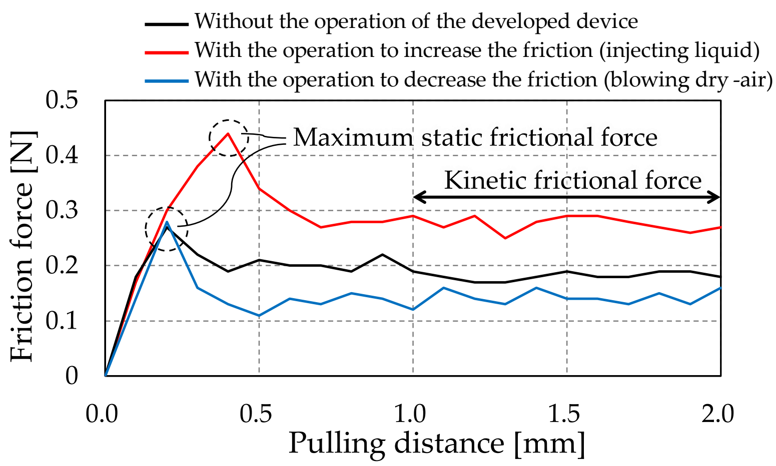

Figure 10. Representative results of the behavior of the friction force under the environmental condition of t20h30.

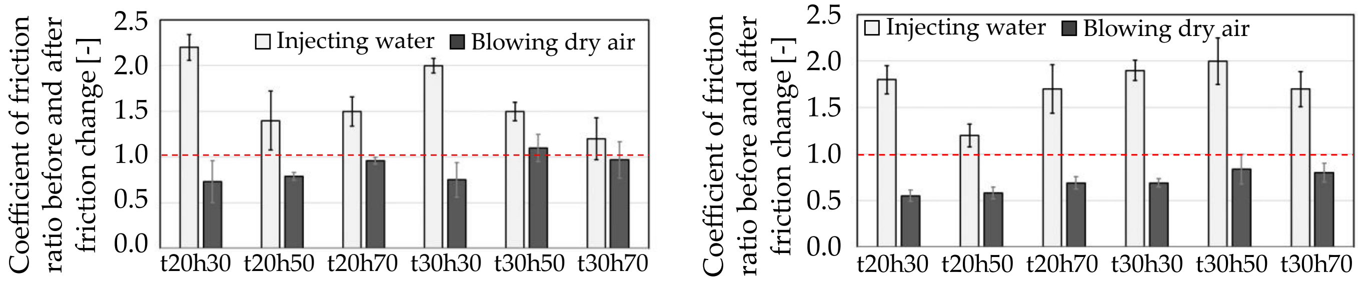

(**a**) (**b**)

Figure 11. Friction coefficient ratios after friction changes through injecting water (white) and blowing dry air (black) over nominal conditions (red line) under different environmental conditions. (**a**) Maximum static friction. (**b**) Kinetic friction.

4.4. Effect of the Granular Objects

This section presents the evaluation of the effect of granular objects inside the pouch. As described in Section 3.1.2, granular objects amplify the function of friction reduction through producing an air pocket around the contact area and maintaining the airflow under external loads. To verify the former role, the maximum static and kinetic friction forces were measured under two conditions: with granular objects inside the pouch (nominal configuration, as shown in Figure 5) and without granular objects. The experimental setup is shown in Figure 9. Experiments were performed through running the device with and without blowing dry air for each configuration (with and without granular objects). The results are expressed as the ratio of the friction coefficients after the friction change (decrease) to those of the nominal case and are presented in Figure 12. The results demonstrate that friction was effectively reduced using the dry-air blowing unit, regardless of the presence of granular objects. The presence of granular objects enhanced the friction reduction.

The experimental setup shown in Figure 13 was used to verify the capability of granular objects to maintain airflow under an external load. When granular objects were used, the tests were performed using the configuration described in Section 2.2, as shown in Figure 13a, where the air tube passed through the pouch of the heating unit, including the granular objects. One side of the tube was connected to the air source, whereas the other side was connected to a flowmeter (8550MC, Kofloc, Kyoto, Japan). For comparison, experiments were also performed without granular objects. In this case, only the air tube was set up, as shown in Figure 13b. The airflow rate from the air source was set to 10 L/min. An external load was applied to the air tube and pouch using a force gauge attached to an automatic positioning stage. The output airflow rate from the air tube was monitored using a flowmeter until the magnitude of the external force reached 25 N. The output airflow rates under both conditions (with and without granular objects) are shown in Figure 14. In the presence of granular objects, the output airflow rate was maintained under an external load. By contrast, the airflow rate decreased under an external load when the air tube did not pass through the pouch containing granular objects. Thus, the results demonstrated the importance of the granular objects in maintaining airflow under external loads.

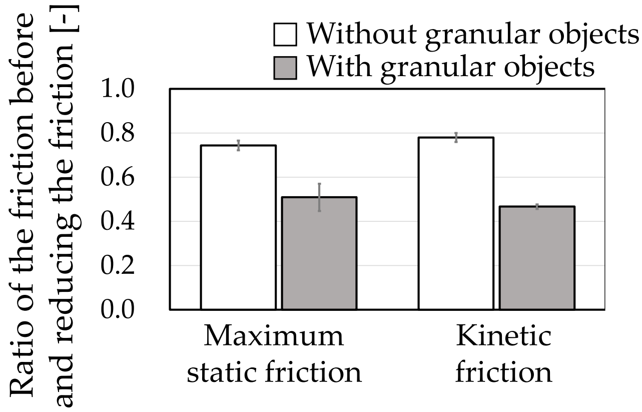

Figure 12. Friction coefficient ratios after friction change to those in the nominal condition, depending on whether the developed device includes granular objects (grey) or not (white).

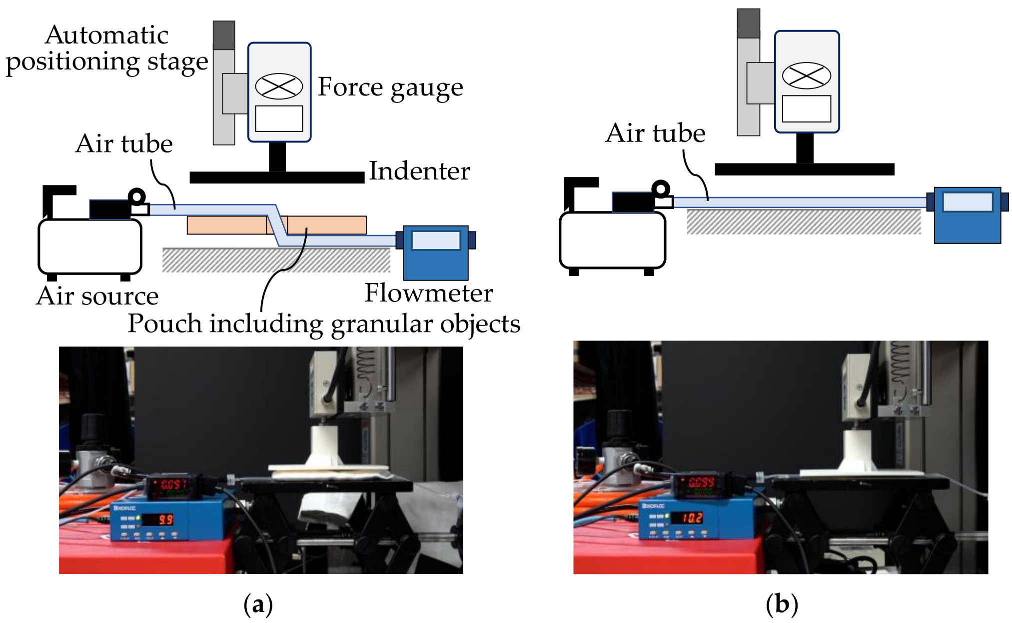

Figure 13. Experimental setup to evaluate the effect of the presence of granular objects under external load: (**a**) with granular objects and (**b**) without granular objects.

4.5. Discussion

This study aimed to develop a device that changes the temperature, humidity, and friction of its surface under different environmental conditions. After experimental validation, the developed device was shown to be effective at tuning these three conditions. The design requirements were satisfied through avoiding the use of electrical motors and attaining a thin structure consisting only of flexible elements.

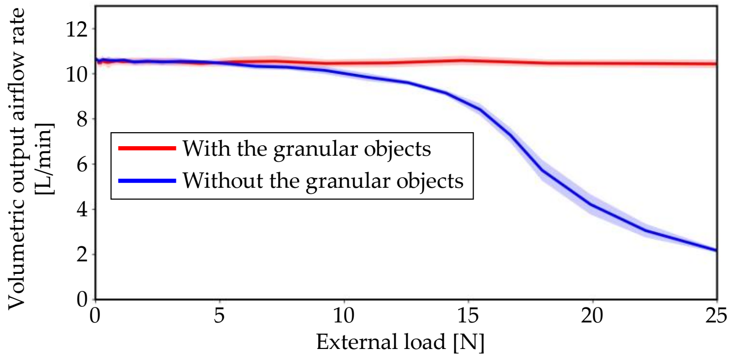

Figure 14. Output volumetric airflow rate under an external load when the air tube passes through the pouch in the presence or absence of granular objects.

The rate of temperature increase measured was approximately 0.44 °C/min, and it could be lowered by more than 1.5 °C after 1 min of water-spraying and 2 min of blowing dry air under any of the environmental conditions tested. Thermal comfort is achieved at temperatures between 28.6 and 32.0 °C [34]; this device takes 10 min to reach thermal comfort when placed in a room at temperatures in the range between 28.6 and 32.0 °C. Thus, the rates of the temperature increase and decrease were deemed sufficient. The optimal relative humidity for healthy skin is approximately 60% RH [35]. Although the extent of humidity change by the device is affected by environmental conditions, the humidity change function could tune humidity sufficiently close to 60% RH. The reduction in kinetic friction achieved by the device is effective for dressing and undressing, whereas the increase in static friction is effective for holding and supporting the human body. The developed variable-friction mechanism satisfied the functions required for the device.

The mechanisms used to tune the temperature, humidity, and friction worked in tandem. Consider a case where the temperature needs to be reduced. If the humidity is high, the dry-air blowing unit decreases both the temperature and humidity; this action also reduces friction, thereby improving garment ventilation. If the humidity is low, both the liquid-injection and dry-air blowing units are activated to decrease the temperature. In this case, to achieve a comfortable humidity level, the humidity should be increased while the temperature is reduced. Thus, the working mechanism of the developed device exhibits good configuration in this context. Increasing the humidity also increases friction, which is generally required when humidity is low. Moreover, when humidity is low, skin moisturization is deemed comfortable, which can be achieved using the liquid-injection function. Conversely, decreasing the humidity also decreases the friction between the device and human skin; both of these are necessary when the humidity is high. Thus, a reduction in friction improves comfort via the ventilation of the worn garments. In summary, the developed device is fully functional and comfortable when used on human skin.

The strategies utilized worked effectively to increase or decrease the temperature, humidity, and friction. However, the environmental conditions of temperature and humidity influence the degree of the increase or decrease. The higher the environmental temperature and the lower the environmental humidity, the higher the degree of temperature cooling. This is owing to the use of vaporization heat for cooling. Moreover, the lower the environmental temperature, the higher the degree of heating. The lower the environmental humidity, the higher the degree of humidification. The higher the environmental temperature and environmental humidity, that is, the higher the environmental absolute humidity, the higher the degree of dehumidification. The lower the environmental humidity, the higher the degree of increase in static friction. However, the difference in degree was small when the environmental humidity was above 50%. This is owing to the use of water injection to increase friction. The lower the environmental absolute humidity, the higher the degree of decrease in static friction. Under conditions t30h70, t30h50, and t20h70, the rate of change was approximately one. This can be attributable to the effect of the amount of ambient water, which is the source of the adhesion force. Moreover, the lower the environmental absolute humidity, the higher the degree of increase and decrease in kinetic friction; this is also attributable to the effect of the amount of ambient water. Table 7 summarizes the correlation coefficients between the varied parameters (temperature, humidity, and friction) and environmental conditions, supporting the above discussion. The amount of change in friction, temperature, and humidity is affected by environmental temperature and humidity and is a limitation of the presented strategy.

Table 7. Correlation coefficients between the varied parameters and environmental conditions.

	Environmental Temperature	Environmental Humidity
Increase in the temperature	−0.98	−0.24
Decrease in the temperature	−0.92	0.24
Increase in the humidity	−0.069	−0.99
Decrease in the humidity	−0.24	−0.97
Increase in the maximum static friction	0.59	−0.24
Decrease in the maximum static friction	0.81	0.49
Increase in the kinetic friction	−0.19	−0.88
Decrease in the kinetic friction	0.42	0.68

5. Installation into Clothes

To test the performance of the developed device when adapted to clothing, an armband incorporating the two developed units was prepared, as shown in Figure 15. Its performance was experimentally evaluated using the setup shown in Figure 16. The armband was wrapped around an acrylic pipe to mimic the human arm. The experiments were conducted under a temperature of 26.9 °C and a relative humidity of 52%.

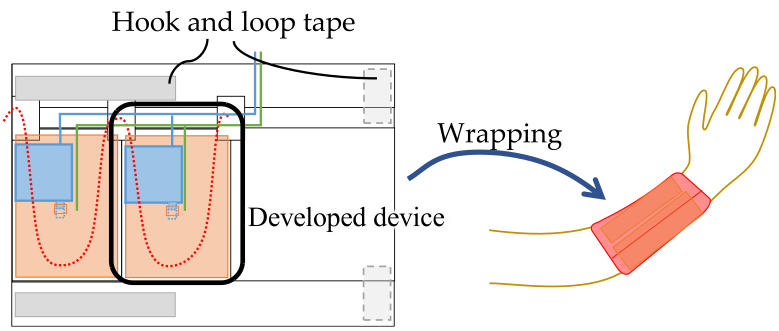

Figure 15. Armband with the developed wearable device.

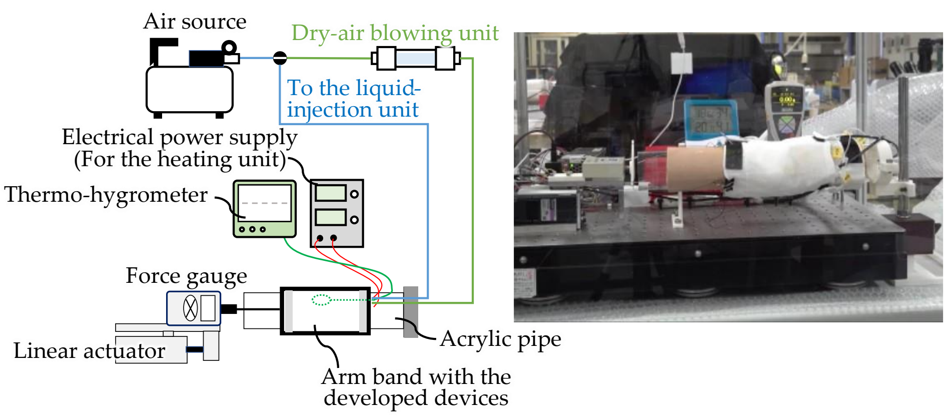

Figure 16. Experimental setup to evaluate the armband containing the developed device.

5.1. Tuning the Temperature

To test temperature tuning, heating and cooling experiments were conducted using an armband. Heating was performed using a heating unit, whereas cooling was performed using liquid-injection and dry-air blowing units. Heating for 7.5 min increased the contact area temperature by 5.0 °C. Cooling via injecting deionized water for 1 min, followed by blowing dry air for 2 min decreased the contact area temperature by 2.6 °C.

5.2. Tuning the Humidity

From the initial condition of the developed device, dry air was blown onto the contact area for 3 min to decrease the humidity. Subsequently, deionized water was sprayed onto the contact area to increase the humidity. Table 8 lists the measurements at each state.

Table 8. Change in humidity when installing the developed device into clothes.

	Initial Condition	Blowing Dry Air	Injecting Water
Relative humidity [%] (Change after installing the device into clothes)	52	33 (−19)	45 (+12)

5.3. Tuning the Friction

Experiments were performed to evaluate the changes in the friction function. The maximum static and kinetic frictions were measured through pulling the armband through the force gauge in the initial condition (device in the OFF position), and through increasing or decreasing the friction using the developed device. To evaluate the increase in friction, the armband was pulled after 1 min of injecting deionized water onto the surface; to evaluate the decrease in friction, the armband was pulled while the dry-air blowing unit was operating. The ratio of the coefficient of friction before and after the friction change was measured, and it is plotted in Figure 17. Thus, the developed device changes the friction on the contact surface as intended. The differences between the results shown in Figure 11 can be explained by differences in the targets.

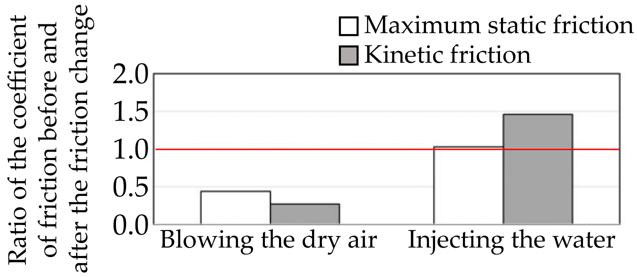

Figure 17. Change in the friction coefficient ratio after blowing dry air and injecting water onto the surface of the developed device over the nominal condition (red line).

6. Conclusions

This study introduced a flexible and thin device that can change its surface properties in terms of temperature, humidity, and friction. The friction change is based on the novel principle of injecting a liquid with a high surface tension onto a surface and creating an air lubrication area surrounded by granular materials to produce the opposite effect. Humidity is increased by means of a liquid-injection unit and decreased by means of a dry-air blowing unit. Cooling is achieved based on the principle of vaporization heat, whereas heating is achieved based on the Joule effect. The performance and effectiveness of the developed device were validated under various environmental conditions. Under the best environmental conditions for temperature change, the temperature of the contact surface increased by 6.6 °C and decreased by 12.0 °C. If a technology providing higher efficiency for the heating wire, such as [36,37], is used, the heating performance would be improved. Under the best environmental conditions for the humidity change, it could be changed between +47% and −48% through injecting water under condition t20h30 and blowing dry air under condition t30h70, respectively. The coefficient of maximum static friction increased by a maximum of 2.2× the reference/nominal condition and decreased to 0.73× the reference/nominal condition. The coefficient of kinetic friction increased by a maximum of 2.0× the reference/nominal condition and decreased to 0.55× the reference/nominal condition. The benefits of granular objects included in the pouch were experimentally validated. Although the experimental results indicate that the strategies utilized to increase or decrease temperature, humidity, and friction work effectively, the environmental conditions of temperature and humidity influence the degree of increase or decrease. This is mainly because the amount of water is varied to change the humidity, lower the temperature, and increase friction: vaporization heating lowered the temperature, and the adhesion force of water increased the friction. The proposed strategy increases and decreases the kinetic friction, and increases the static friction, the extent of which is influenced by the absolute humidity of the environment. The absolute humidity of the environment has a strong effect when lowering the static friction; essentially, the change in static friction changed little when the absolute humidity was high. A garment incorporating the developed device was fabricated and its performance was evaluated. The device attached to the garment changed its state (temperature, humidity, and friction) in the same manner as the stand-alone mechanisms. In this paper, the actuation was conducted manually. Future work will focus on the development and evaluation of further garments to cover the human trunk, such as T-shirts, and a control system based on sensor information. A physical analysis of the proposed principles and design optimization based on this analysis will also be conducted in our future work.

Author Contributions: Conceptualization, T.W.; methodology, S.N., K.T. and T.W.; software, S.N.; validation, T.N., N.K., Y.H. and T.W.; formal analysis, T.N., Y.H. and T.W.; investigation, N.K. and Y.H.; resources, T.W.; data curation, T.W.; writing—original draft preparation, T.N.; writing—review and editing, T.W. and K.T.; supervision, T.W.; project administration, T.N. and T.W.; funding acquisition, T.W. All authors have read and agreed to the published version of the manuscript.

Funding: This work was partially supported by JST [Moonshot R&D] [Grant Number JPMJMS2034].

Institutional Review Board Statement: Not applicable.

Informed Consent Statement: Not applicable.

Data Availability Statement: Not applicable.

Conflicts of Interest: The authors declare no conflict of interest.

References

1. Stevens, K.; Fuller, M. *Textile-Led Design for the Active Ageing Population*; Elsevier: Amsterdam, The Netherlands, 2015; ISBN 9780857095381.
2. Havenith, G. Interaction of Clothing and Thermoregulation. *Exog. Dermatol.* **2002**, *1*, 221–230. [CrossRef]
3. Sanchez, V.; Walsh, C.J.; Wood, R.J. Textile Technology for Soft Robotic and Autonomous Garments. *Adv. Funct. Mater.* **2021**, *31*, 2008278. [CrossRef]
4. Okui, M.; Nagura, Y.; Iikawa, S.; Yamada, Y.; Nakamura, T. A Pneumatic Power Source Using a Sodium Bicarbonate and Citric Acid Reaction with Pressure Booster for Use in Mobile Devices. In Proceedings of the 2017 IEEE/RSJ International Conference on Intelligent Robots and Systems (IROS), Vancouver, BC, Canada, 24–28 September 2017; IEEE: New York, NY, USA; pp. 1040–1045.
5. Hu, R.; Liu, Y.; Shin, S.; Huang, S.; Ren, X.; Shu, W.; Cheng, J.; Tao, G.; Xu, W.; Chen, R.; et al. Emerging Materials and Strategies for Personal Thermal Management. *Adv. Energy Mater.* **2020**, *10*, 1903921. [CrossRef]
6. Kotagama, P.; Phadnis, A.; Manning, K.C.; Rykaczewski, K. Rational Design of Soft, Thermally Conductive Composite Liquid-Cooled Tubes for Enhanced Personal, Robotics, and Wearable Electronics Cooling. *Adv. Mater. Technol.* **2019**, *4*, 1800690. [CrossRef]
7. Guo, T.; Shang, B.; Duan, B.; Luo, X. Design and Testing of a Liquid Cooled Garment for Hot Environments. *J. Therm. Biol.* **2015**, *49*, 47–54. [CrossRef]
8. Mondal, S. Phase Change Materials for Smart Textiles—An Overview. *Appl. Therm. Eng.* **2008**, *28*, 1536–1550. [CrossRef]

9. Bühler, M.; Popa, A.M.; Scherer, L.J.; Lehmeier, F.K.S.; Rossi, R.M. Heat Protection by Different Phase Change Materials. *Appl. Therm. Eng.* **2013**, *54*, 359–364. [CrossRef]
10. Wang, R.; Xu, Z.; Zhuang, J.; Liu, Z.; Peng, L.; Li, Z.; Liu, Y.; Gao, W.; Gao, C. Highly Stretchable Graphene Fibers with Ultrafast Electrothermal Response for Low-Voltage Wearable Heaters. *Adv. Electron. Mater.* **2017**, *3*, 1600425. [CrossRef]
11. Guo, Y.; Dun, C.; Xu, J.; Mu, J.; Li, P.; Gu, L.; Hou, C.; Hewitt, C.A.; Zhang, Q.; Li, Y.; et al. Ultrathin, Washable, and Large-Area Graphene Papers for Personal Thermal Management. *Small* **2017**, *13*, 1702645. [CrossRef]
12. Zhang, L.; Baima, M.; Andrew, T.L. Transforming Commercial Textiles and Threads into Sewable and Weavable Electric Heaters. *ACS Appl. Mater. Interfaces* **2017**, *9*, 32299–32307. [CrossRef]
13. Choi, J.; Dun, C.; Forsythe, C.; Gordon, M.P.; Urban, J.J. Lightweight Wearable Thermoelectric Cooler with Rationally Designed Flexible Heatsink Consisting of Phase-Change Material/Graphite/Silicone Elastomer. *J. Mater. Chem. A* **2021**, *9*, 15696–15703. [CrossRef]
14. Kishore, R.A.; Nozariasbmarz, A.; Poudel, B.; Sanghadasa, M.; Priya, S. Ultra-High Performance Wearable Thermoelectric Coolers with Less Materials. *Nat. Commun.* **2019**, *10*, 1765. [CrossRef]
15. Zaia, E.W.; Gordon, M.P.; Yuan, P.; Urban, J.J. Progress and Perspective: Soft Thermoelectric Materials for Wearable and Internet-of-Things Applications. *Adv. Electron. Mater.* **2019**, *5*, 1800823. [CrossRef]
16. Panasonic Corporation. Available online: https://www.na.panasonic.com/ (accessed on 6 June 2023).
17. Sharp Electronics Corporation. Available online: https://www.sharpusa.com/ (accessed on 6 June 2023).
18. Suzuki, K.; Ohzono, T. Wrinkles on a Textile-Embedded Elastomer Surface with Highly Variable Friction. *Soft Matter* **2016**, *12*, 6176–6183. [CrossRef] [PubMed]
19. Liu, D.; Broer, D.J. Self-Assembled Dynamic 3D Fingerprints in Liquid-Crystal Coatings Towards Controllable Friction and Adhesion. *Angew. Chemie* **2014**, *126*, 4630–4634. [CrossRef]
20. Glick, P.; Suresh, S.A.; Ruffatto, D.; Cutkosky, M.; Tolley, M.T.; Parness, A. A Soft Robotic Gripper with Gecko-Inspired Adhesive. *IEEE Robot. Autom. Lett.* **2018**, *3*, 903–910. [CrossRef]
21. Golan, Y.; Shapiro, A.; Rimon, E. Jamming-Free Immobilizing Grasps Using Dual-Friction Robotic Fingertips. *IEEE Robot. Autom. Lett.* **2020**, *5*, 2889–2896. [CrossRef]
22. Abdi, H.; Asgari, M.; Nahavandi, S. Active Surface Shaping for Artificial Skins. In Proceedings of the 2011 IEEE International Conference on Systems, Man, and Cybernetics, Anchorage, AK, USA, 9–12 October 2011; IEEE: New York, NY, USA; pp. 2910–2915.
23. Nojiri, S.; Mizushima, K.; Suzuki, Y.; Tsuji, T.; Watanabe, T. Development of Contact Area Variable Surface for Manipulation Requiring Sliding. In Proceedings of the 2019 2nd IEEE International Conference on Soft Robotics (RoboSoft), Seoul, Republic of Korea, 14–18 April 2019; IEEE: New York, NY, USA; pp. 131–136.
24. Becker, K.P.; Bartlett, N.W.; Malley, M.J.D.; Kjeer, P.M.; Wood, R.J. Tunable Friction through Constrained Inflation of an Elastomeric Membrane. In Proceedings of the 2017 IEEE International Conference on Robotics and Automation (ICRA), Singapore, 29 May–3 June 2017; IEEE: New York, NY, USA; pp. 4352–4357.
25. Spiers, A.J.; Calli, B.; Dollar, A.M. Variable-Friction Finger Surfaces to Enable Within-Hand Manipulation via Gripping and Sliding. *IEEE Robot. Autom. Lett.* **2018**, *3*, 4116–4123. [CrossRef]
26. Lu, Q.; Clark, A.B.; Shen, M.; Rojas, N. An Origami-Inspired Variable Friction Surface for Increasing the Dexterity of Robotic Grippers. *IEEE Robot. Autom. Lett.* **2020**, *5*, 2538–2545. [CrossRef]
27. Kim, S.; Sitti, M.; Xie, T.; Xiao, X. Reversible Dry Micro-Fibrillar Adhesives with Thermally Controllable Adhesion. *Soft Matter* **2009**, *5*, 3689. [CrossRef]
28. Shintake, J.; Rosset, S.; Schubert, B.; Floreano, D.; Shea, H. Versatile Soft Grippers with Intrinsic Electroadhesion Based on Multifunctional Polymer Actuators. *Adv. Mater.* **2016**, *28*, 231–238. [CrossRef] [PubMed]
29. Hawkes, E.W.; Christensen, D.L.; Han, A.K.; Jiang, H.; Cutkosky, M.R. Grasping without Squeezing: Shear Adhesion Gripper with Fibrillar Thin Film. In Proceedings of the 2015 IEEE International Conference on Robotics and Automation (ICRA), Seattle, WA, USA, 26–30 May 2015; IEEE: New York, NY, USA, 2015; pp. 2305–2312.
30. Mizushima, K.; Suzuki, Y.; Tsuji, T.; Watanabe, T. Deformable Fingertip with a Friction Reduction System Based on Lubricating Effect for Smooth Operation under Both Dry and Wet Conditions. *Adv. Robot.* **2019**, *33*, 508–519. [CrossRef]
31. Nishimura, T.; Shimizu, K.; Nojiri, S.; Tadakuma, K.; Suzuki, Y.; Tsuji, T.; Watanabe, T. Soft Robotic Hand with Finger-Bending/Friction-Reduction Switching Mechanism Through 1-Degree-of-Freedom Flow Control. *IEEE Robot. Autom. Lett.* **2022**, *7*, 5695–5702. [CrossRef]
32. Nishi, T.; Moriyasu, K.; Harano, K.; Nishiwaki, T. Influence of Dewettability on Rubber Friction Properties with Different Surface Roughness under Water/Ethanol/Glycerol Lubricated Conditions. *Tribol. Online* **2016**, *11*, 601–607. [CrossRef]
33. Nojiri, S.; Nishimura, T.; Tadakuma, K.; Watanabe, T. Flexible and Slim Device Switching Air Blowing and Suction by a Single Airflow Control. *IEEE Robot. Autom. Lett.* **2023**, *8*, 2637–2644. [CrossRef]
34. Kwon, J.; Choi, J. Clothing Insulation and Temperature, Layer and Mass of Clothing under Comfortable Environmental Conditions. *J. Physiol. Anthropol.* **2013**, *32*, 11. [CrossRef]
35. Dermidia, DSI Sense. Available online: https://dermidia.com/what-indoor-humidity-is-the-optimum-level-for-healthy-skin/ (accessed on 6 June 2023).

36. Chen, X.-Q.; Fan, S.-J.; Han, C.; Wu, T.; Wang, L.-J.; Jiang, W.; Dai, W.; Yang, J.-P. Multiscale Architectures Boosting Thermoelectric Performance of Copper Sulfide Compound. *Rare Met.* **2021**, *40*, 2017–2025. [CrossRef]
37. Chen, X.; Zhang, H.; Zhao, Y.; Liu, W.-D.; Dai, W.; Wu, T.; Lu, X.; Wu, C.; Luo, W.; Fan, Y.; et al. Carbon-Encapsulated Copper Sulfide Leading to Enhanced Thermoelectric Properties. *ACS Appl. Mater. Interfaces* **2019**, *11*, 22457–22463. [CrossRef]